JOM, Vol. 66, No. 7, 2014
DOI: 10.1007/s11837-014-0981-4

Research on the Penetration Depth in Aluminum Reduction Cell with New Type of Anode and Cathode Structures

LIU YAN,[1] LI YUDONG,[1,2] ZHANG TING'AN,[1] and FENG NAIXIANG[1]

1.—Key Laboratory of Ecological Utilization of Multi-Metal Intergrown Ores of Education Ministry, School of Materials and Metallurgy of Northeastern University, Shenyang 110004, People's Republic of China. 2.—e-mail: liyudong1@hotmail.com

In this article, a cold water model experiment based on the principle of similitude was conducted to study penetration depth and to investigate the rules of penetration depth (the thickness of bubble sheet) in new anode structure electrolytic cell. New structure anodes and new structure cathodes were designed to examine penetration depth induced by anodic gas in the electrolytic cell. A high-speed camera was used to take photographs of the water model experiment. After that, photographs were analyzed by Image-Pro Plus software. The results revealed the effect of different parameters such as slit width, anode–cathode distance, electrolyte level, and gas rate on the penetration depth. The results provide several meaningful suggestions in selecting electrolysis apparatus. Finally, through dimensional analyzing, the penetration depth criterion equation of the 1/2 anode structure electrolytic cell was obtained. In sum, water model experimental results provide theoretical and experimental basis for the new anode structure and new cathode structure electrolysis cell's design and practice.

INTRODUCTION

To save energy in the aluminum electrolysis industry and to promote the basic theory research of the new structure of aluminum reduction cell, with the support of National Natural Science Foundation and the "863 Project," based on the cathode and anode structure of new structure cell and the scientific theory of process and technical operation, Northeastern University studies the influence of new structure on the fluctuations of aluminum liquid systematically and developed a scientific theory that realizes minimum fluctuation in the process of aluminum electrolysis in new cathode structure cell.[1–3] We have established a scientific theory about new structure aluminum electrolytic cell to ensure that the cathode aluminum liquid has the smallest fluctuations.

Research is lacking on the penetration depth's influence on the electrolysis process based on the new structure aluminum electrolyte cell. No one has ever researched on the different structure anode's effects on the penetration depth. The optimal combination of new anode and new cathode are of industrial value, but no one has researched that from a theoretical and experimental perspective.

Figure 1 shows that polar distance (h) is formed by the aluminum liquid fluctuation layer (a), the mixed layer of bubble and electrolyte (b), and the intermediate electrolyte transition layer (c).[4] The width of the mixed layer (b) is defined as the penetration depth. Obviously, we can obtain the equation:

$$h = a + b + c$$

In this experiment, we researched the influence on the penetration depth (b) by different anode and cathode structure. Through the research on the mixed layer (b), we drew a comparison of the influence of different operating conditions. To decrease the polar distance, much research has been conducted on the aluminum liquid fluctuation layer (a) to reduce the interface fluctuation. But almost no one has done any research on the mixed layer (b). Considering the current situation of the aluminum electrolysis, this article focuses on the investigation of the mixed layer (b). This work manages to

(Published online May 21, 2014)

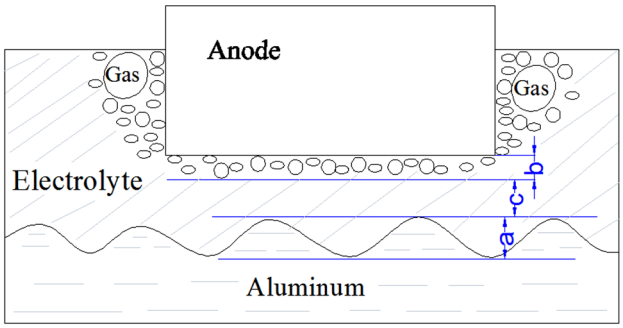

Fig. 1. Polar distance model constructed by three layers.

Table I. A comparison between model and cell data

Parameter (mm)	Prototype cell	Model
Size of anodes	1520 × 585 × 535	506 × 195 × 178
Size of cell	8945 × 4220 × 600	2981 × 1406 × 600

minimize the polar distance by reducing the penetration depth.

EXPERIMENTAL PRINCIPLE AND EQUIPMENT

Experimental Model

To make predictions relevant to the industrial cell, the model used should have both geometrical similarity (i.e., similar relationships in main dimensions) and dynamical similarity (i.e., similar relationships between forces).

Geometrical Similarity

The experiment model and the industrial aluminum electrolytic cell have the same proportion in main dimensions, but the model is smaller than the prototype. Based on the practical field production situation, the aluminum electrolysis process is investigated, and data are collected regarding the aluminum cell size and production operating parameters.[5–7] The rate between the experimental model and the prototype is 1:3, and in the experiment, the new structure cathode and new structure anode are made by synthetic glass based on the rate. The corresponding data of the model and prototype cell are listed in Table I and the physical model photograph is shown in Fig. 2.

There are four new anode structures in this experiment: 1/2 anode with chamfer, 1/2 anode without chamfer, 1/4 anode with chamfer, and 1/4 anode without chamfer. The 1/2 anode has a slit at the short edge that divided the whole anode into two parts. In the experiment, we constructed three 1/2 anodes with different slit widths. They were,

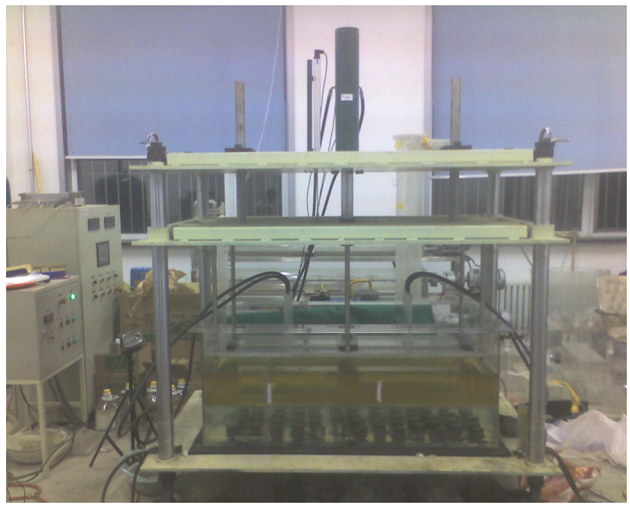

Fig. 2. Physical model photograph.

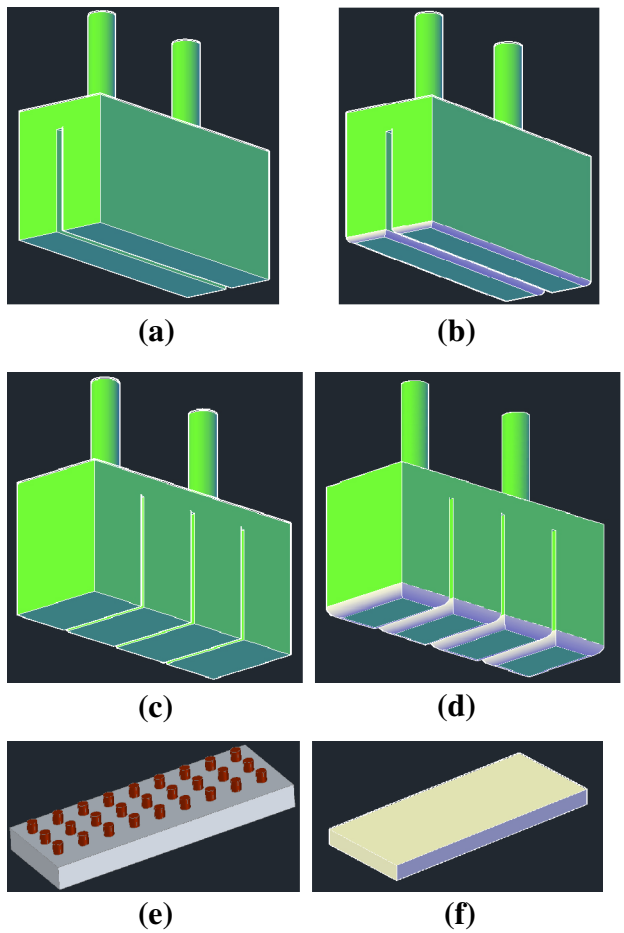

Fig. 3. Anode structures (a, b, c, and d) and Cathode structures (e and f), (a) 1/2 anode without chamfer, (b) 1/2 anode with chamfer, (c) 1/4 anode without chamfer, (d) 1/4 anode with chamfer, (e) new cathodes structure, and (f) normal cathode structure.

respectively, 5 mm, 10 mm, and 15 mm. The new structures of anode and cathode are shown in Fig. 3.

Table II. Comparison between cell and model data

Parameter	Model	Cell
ρ_b, kg/m^3	0.9	2.1
ρ_m, kg/m^3	1.0	2.3
v_b, mm^2/s	2.7	1.3
v_m, mm^2/s	1.0	0.4
σ_{b-m}, N/m	0.03	0.55
σ_{b-g}, N/m	0.02	0.14

Dynamic Similarity

The physical properties of the fluids in an industrial cell are unfortunately difficult to match. The molten metal phase in industrial cells has a low viscosity and a high surface tension—which is not easily obtainable with commonly used cold fluids. In the current model, water is used to simulate the metal phase, light vegetable oil is used for the bath, and air is used for the gas formed under the anode. The oil–water combination was chosen to match the density and viscosity ratios as closely as possible, using safe and inexpensive room-temperature fluids to guarantee dynamical similarity. A summary of the relevant parameters, compared with the industrial cell parameters, is given in Table II.

In this article, combined with experiments' results and results of previous research, the major influence factors of penetration depth were analyzed and summarized. For some similar processes, they must maintain the similarity criteria and have the same control equation. By analyzing the experimental data, the empirical formula of penetration depth was obtained using dimensional analysis, which is related to the kinds of material factors, operating factors and equipment factors.

RESULTS AND DISCUSSION

Effect of 1/4 Anode's Slit Width, Anode's Chamfer, and Cathode's Structure on Penetration Depth

The experiment conditions are as follows. The cathode–anode distance (d) was 30 mm. The electrolyte level (h) was 160 mm. The aluminum level was 170 mm. The gas flow rate (Q) was 1.5 m^3/h.

This experiment focused on the 1/4 anode. Several 1/4 anodes with different slit widths (W) were used: 5 mm, 10 mm, and 20 mm, respectively. Also, this experiment investigated the effect of anode's chamfer and cathode's structure on penetration depth.

Experiments were recorded by a digital camera at 40 frames per second, and the actual measurements were done on a computer after rescaling the images according to a metric ruler fixed to the apparatus. The photographs are shown in Fig. 4. These photographs were analyzed, the results are listed in Table III.

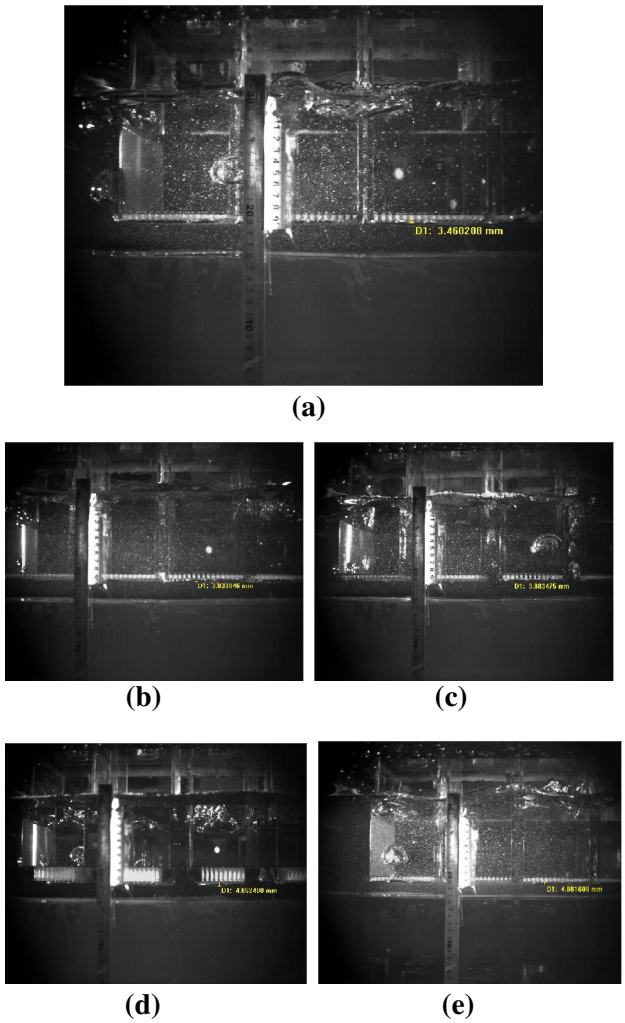

Fig. 4. Photographs (after analysis) of the experiment phenomenon using 1/4 anodes, (a) $W = 5$ mm, without chamfer and normal cathode; (b) 10 mm, without chamfer and normal cathode; (c) 20 mm, without chamfer and normal cathode; (d) 20 mm, with chamfer and normal cathode; and (e) 20 mm, without chamfer and new cathode.

Table III. A summary of penetration depth (A) under 1/4 anode

No.	W (mm)	Chamfer	Cathode structure	A (mm)
a	5	No	Normal	3.460208
b	10	No	Normal	3.833846
c	20	No	Normal	3.883475
d	20	Yes	Normal	4.062480
e	20	No	New	4.081609

Conclusions of this series experiments are stated as follows:

1. Considering the statistics in Table I, taking a, b, and c experiments into account, anodes with

large slit widths in the range 5–20 mm have a greater penetration depth than anodes with small slit widths.
2. Comparing the statistics in experiment c and d, we can see that anodes with chamfer may cause larger penetration depth than that of anodes without chamfer. As time passes, the chamfer corroded by the electrolyte will be larger. This reveals that after using them with a larger chamfer for a long time, the anodes will cause a larger penetration depth.
3. Taking experiments c and e into account, the statistics show that the normal cathode structure can be more desirable than that of the new cathode structure in decreasing the penetration depth.

Effect of 1/2 Anode's Slit Width (*W*) on Penetration Depth

The experiment conditions are as follows. The slit widths of anodes were 5 mm, 10 mm, and 15 mm, respectively. The gas flow rates were 0.9 m^3/h, 1.2 m^3/h, and 1.5 m^3/h. The anode–cathode distance was 30 mm. The electrolyte level was 160 mm. The aluminum level was 170 mm.

After recording and analyzing the experiment photographs as in Experiment 3.1, the results are shown in Table IV.

The conclusions derived from statistics in Table IV are stated as follows: The increase of gas flow rate has a positive influence on the penetration depth. Under different gas flow rates, the increase of slit widths (from 5 mm to 15 mm) can cause an increase in the penetration depth. Taking both Experiment 1 and Experiment 2 into account, a smaller slit width in an appropriate range is satisfactory in decreasing the penetration depth, whether the anode structure is 1/2 anode or 1/4 anode.

Effect of Different Cathode Structures on Penetration Depth Using 1/2 Anode

The experiment conditions are as follows. The gas flow rates were 0.9 m^3/h, 1.2 m^3/h, and 1.5 m^3/h. The anode–cathode distance was 30 mm. The slit width of the 1/2 anode was 15 mm. The electrolyte level was 160 mm. The aluminum level was 170 mm.

After recording and analyzing the experiment photographs as Experiment 3.1, the results are shown in Table V.

The comparison between two groups of experiments shows that the usage of a new structure cathode can cause an increase of the penetration depth. Taking both Experiment 1 and Experiment 3 into account, the new cathode structure is not preferred in decreasing penetration depth no matter what the anode structure is.

Table IV. A summary of penetration depth (*A*) under 1/2 anode with different slit width (*W*)

	A (mm)		
Q (m^3/h)	*W* = 5 mm	*W* = 10 mm	*W* = 15 mm
0.9	2.875399	3.02115	3.29340
1.2	3.205128	3.63635	3.97553
1.5	3.571429	3.89222	4.25530

Table V. A summary of penetration depth (*A*) under 1/2 anode using different cathode structures

	A (mm)	
Q (m^3/h)	New cathode	Normal cathode
0.9	3.559871	3.293398
1.2	4.234528	3.975535
1.5	4.516129	4.255299

Table VI. A summary of penetration depth under different anodes

	A (mm)	
W (mm)	1/2 Anode	1/4 Anode
5	3.571429	3.460208
10	3.89222	3.833846

Comparison of the 1/2 Anode's and 1/4 Anode's Effect on Penetration Depth

The experiment conditions are as follows. The anode–cathode distance was 30 mm. The electrolyte level was 160 mm. The aluminum level was 170 mm. The gas flow rate was 1.5 m^3/h. Four anodes were used in this experiment: 1/2 anode with 5-mm slit, 1/2 anode with 10-mm slit, 1/4 anode with 5-mm slit, and 1/4 anode with 10-mm slit.

After recording and analyzing the experiment photographs as Experiment 3.1, the results are listed in Table VI.

A conclusion derived from the statistics in Table VI is that the 1/4 anode can minimize the penetration depth more than the 1/2 anode. Compared with the 1/2 anode, the 1/4 anode was divided into more separate parts, which means that it has less separate bottom face area, which may be the reason why the 1/4 anode seemed to be more desirable in decreasing the penetration depth.

Dimensional Analysis in Penetration Depth of New Structure of Aluminum Electrolytic Cells

The Major Influence Factors That Affected Penetration Depth A in Aluminum Electrolytic Cells

Through the analysis of experimental data, we know the penetration depth A is affected mainly by the following factors:

1. A increases with the increase of gas flow rate Q, that is $A \propto Q^a$.
2. A decreases with the increase of polar distance d, $A \propto d^b$.
3. A decreases with the increase of the electrolyte level h, that is $A \propto h^c$.
4. Summarizing previous research on polar distance, we confirm that the penetration depth is also related to the density difference between water and oil $\triangle\rho$, the aluminum liquid level H, water–oil surface tension σ, the viscosity of water μ_1, the viscosity of the oil μ_2, and other factors, but they are constant in this experiment, so we would not give a detailed discussion.

From the analysis above, using dimensional analysis methods, the general function form can be drawn as follows:

$$A = f(Q, H, h, d, \Delta\rho, \mu_1, \mu_2, \sigma, g)$$

Or:

$$f(A, Q, H, h, d, \Delta\rho, \mu_1, \mu_2, \sigma, g) = 0 \qquad (1)$$

Several variables are listed in Table VII.

Establishment of the Dimensionless Formula of Undetermined Parameter

According to the π theorem, the total numbers of variable n = 10 and number of independent variable k = 3 are known in this article. We can create $n-k$ = 7 dimensionless parameter combinations. After the analysis, we selected H, σ, and $\triangle\rho$ as independent variables. Then, variables A, h, and d only contain dimensionless lengths. So their constructor of dimensionless π theorem can be expressed with the independent variable H only. All of the seven π can be expressed as:

$$\pi_0 = H^{\alpha_0}\sigma^{\beta_0}\Delta\rho^{\gamma_0}Q$$
$$\pi_1 = H^{\alpha_1}\sigma^{\beta_1}\Delta\rho^{\gamma_1}\mu_1$$
$$\pi_2 = H^{\alpha_2}\sigma^{\beta_2}\Delta\rho^{\gamma_2}\mu_2$$
$$\pi_3 = H^{\alpha_3}\sigma^{\beta_3}\Delta\rho^{\gamma_3}g$$
$$\pi_4 = \frac{A}{H}$$
$$\pi_5 = \frac{h}{H}$$
$$\pi_6 = \frac{d}{H}$$

For π_0, dimensionless relationship can be obtained into various dimensionless variables:

$$\left[M^0L^0T^0\right] = [L]^{\alpha_0}\left[MT^{-2}\right]^{\beta_0}\left[ML^{-3}\right]^{\gamma_0}\left[L^3T^{-1}\right] \qquad (2)$$

so:

$$M:\ 0 = \beta_0 + \gamma_0$$
$$L:\ 0 = \alpha_0 - 3\gamma_0 + 3$$
$$T:\ 0 = -2\beta_0 - 1$$

Solve for: α_0 = –3/2, β_0 = −1/2, γ_0 = 1/2, so:

$$\pi_0 = H^{-\frac{3}{2}}\sigma^{-\frac{1}{2}}\Delta\rho^{\frac{1}{2}}Q$$

Also it can be written as:

$$\pi_0 = \frac{\Delta\rho Q^2}{H^3\sigma}$$

Similarly:

$$\pi_1 = \frac{\mu_1^2}{H\sigma\Delta\rho}, \quad \pi_2 = \frac{\mu_2^2}{H\sigma\Delta\rho}, \quad \pi_3 = \frac{H^2\Delta\rho g}{\sigma}$$

Put them into Eq 1 to obtain Eq 3:

$$f\left(\frac{\Delta\rho Q^2}{H^3\sigma}, \frac{\mu_1^2}{H\sigma\Delta\rho}, \frac{\mu_2^2}{H\sigma\Delta\rho}, \frac{H^2\Delta\rho g}{\sigma}, \frac{A}{H}, \frac{d}{H}, \frac{h}{H}\right) = 0 \qquad (3)$$

Table VII. Dimensions of variables

	A	Q	h	d	H	μ_1	μ_2	$\triangle\rho$	σ	g
M	0	0	0	0	0	1	1	1	1	0
L	1	3	1	1	1	−1	−1	−3	0	1
T	0	−1	0	0	0	−1	−1	0	−2	−2

It can be also written as a form of the following explicit function:

$$\frac{A}{H}=f\left(\frac{\Delta\rho Q^2}{H^3\sigma},\frac{\mu_1^2}{H\sigma\Delta\rho},\frac{\mu_2^2}{H\sigma\Delta\rho},\frac{H^2\Delta\rho g}{\sigma},\frac{d}{H},\frac{h}{H}\right) \quad (4)$$

Concerning H, $\triangle\rho$, μ_1, σ, μ_2, and g are quantitative, so:

$$\frac{A}{H}=kf\left(\frac{\Delta\rho Q^2}{H^3\sigma},\frac{d}{H},\frac{h}{H}\right)$$

The specific changes of $f\left(\frac{\Delta\rho Q^2}{H^3\sigma},\frac{d}{H},\frac{h}{H}\right)$ is based on the following three variables:

$$\frac{\Delta\rho Q^2}{H^3\sigma},\frac{d}{H},\frac{h}{H}$$

They need to be determined by experiments.

Determination of the Dimensionless Equation

According to the Eq 4 and experimental results, an empirical formula could be established. In this work, different structures of anodes and cathodes had the same form of the formula based on the dimensional analysis, but the results of empirical formula were different.

The empirical formula could be expressed as a power function containing arguments within a certain range. The empirical formula could be expressed as follows:

$$\frac{A}{H}=K\left(\frac{\Delta\rho Q^2}{H^3\sigma}\right)^x\left(\frac{d}{H}\right)^y\left(\frac{h}{H}\right)^z \quad (5)$$

where K, x, y, and z were the fitting coefficients.

Making the logarithmic transformation of Eq 5 could get Eq 6.

$$\ln\frac{A}{H}=\ln K+x\ln\frac{\Delta\rho Q^2}{H^3\sigma}+y\ln\frac{d}{H}+z\ln\frac{h}{H} \quad (6)$$

According to Eq. 4 and experimental results, the value of the fitting coefficients could be obtained as follows:

$$K=0.0005439,\quad x=0.236055,$$
$$y=-0.268231,\ \text{and}\quad z=1.782124$$

So:

$$\frac{A}{H}=0.0005439\left(\frac{\Delta\rho Q^2}{H^3\sigma}\right)^{0.236055}\left(\frac{d}{H}\right)^{-0.268231}\left(\frac{h}{H}\right)^{1.782124} \quad (7)$$

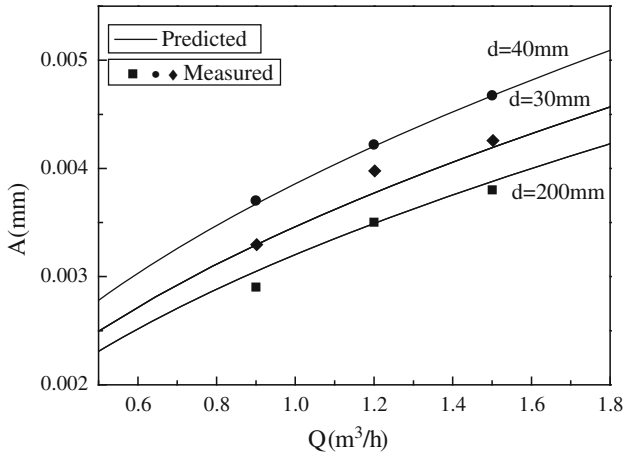

Fig. 5. Comparison between the measured and the predicted penetration depth.

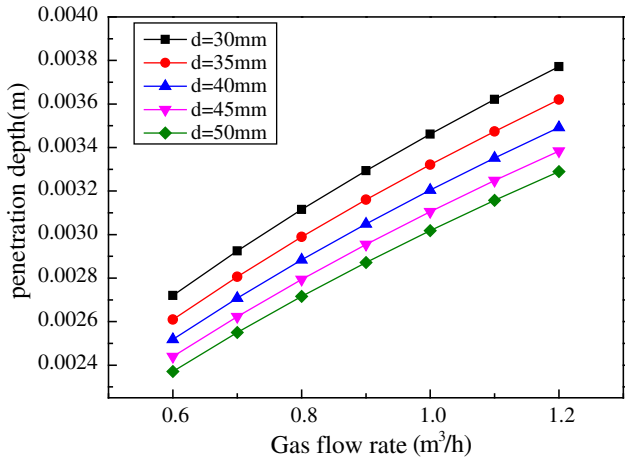

Fig. 6. Effects of gas flow on penetration depth under different anode–cathode distances.

The value calculated by Eq 7 was compared with the experimental results in Fig. 5. The comparison of measured and predicted value showed a great coincidence between the experiment and the dimensionless formula. Thus, the formula is creditable in predicting the penetration depth under different operation condition.

Analysis and Discussion of Dimensionless Equation with Penetration Depth

Effects of Gas Flow on Penetration Depth under Different Polar Distances

The following assumptions were made: The aluminum liquid level H is 170 mm, the electrolyte level h is 160 mm, the surface tension σ is 0.02 N/m, and the density difference between oil and water $\triangle\rho$ is 100 kg/m^3. The following formula was obtained:

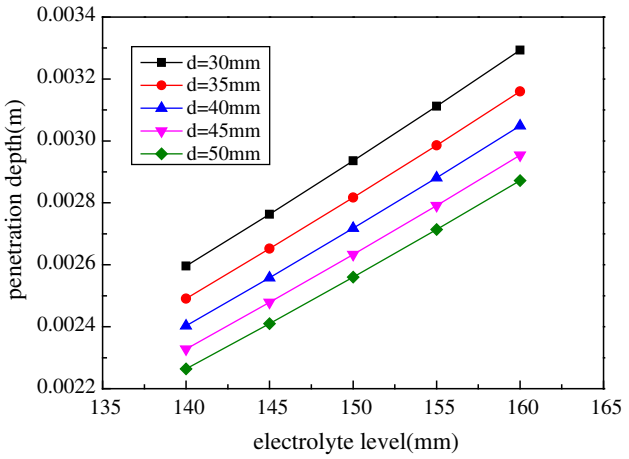

Fig. 7. Effects of electrolyte level on penetration depth under different polar distances.

$$A = 0.001351Q^{0.47211}d^{-0.268231} \quad (8)$$

Figure 6 showed that under different polar distances, the penetration depth increased after the gas flow rate increased. This phenomenon showed that when the polar distance was constant, a higher gas flow rate could increase the penetration depth possibly because the anode gas cannot release immediately after the gas was formed under the anode. Then the high gas flow rate may cause more gas to be attached under the anode than the low gas flow rate. The anode bubble sheet contributes to the increase of the penetration depth.

Effects of Electrolyte Level on Penetration Depth under Different Polar Distances

The following assumptions were made: The aluminum liquid level H is 170 mm, gas flow rate Q = 0.9 m^3/h, the surface tension σ is 0.02 N/m, and the density difference between oil and water $\triangle\rho$ is 100 kg/m^3. The following formula was obtained:

$$A = 0.034539d^{-0.268231}h^{1.782124} \quad (9)$$

Figure 7 shows that under different polar distances, the penetration depth increases after the electrolyte level rate increases. This phenomenon showed that when the polar distance was constant, a higher electrolyte level could decrease the penetration depth possibly because a higher electrolyte level caused a higher pressure under the anode. Bubble sheets under anode were not easy to release under high pressure.

Effect of Polar Distance on Penetration Depth

Figures 6 and 7 show that under the same conditions (besides polar distance), the penetration depth decreases when the polar distance increases. This result is in accord with the objective reality. As our target is to decrease the polar distance, this result shows that we decreased the penetration depth to decrease the polar distance.

CONCLUSION

In this experiment, a cold water model was constructed to study the influence of different anode and cathode structures on the penetration depth. The polar distance of new structure aluminum electrolysis cell had almost achieved the minimum, and cell voltage still could not be reduced greatly. To solve this crucial problem, research on the mixed layer of bubbles was proposed. This research optimized the electrolysis process by reducing penetration depth.

After analyzing and summarizing the results of this experiment, the following conclusions below are made:

1. A smaller slit width in an appropriate range is satisfactory in decreasing penetration depth, whether the anode structure is 1/2 anode or 1/4 anode.
2. The new cathode structure is not preferred in decreasing penetration depth no matter what the anode structure is.
3. Compared with the 1/2 anode, the 1/4 anode with a same slit is more desirable in decreasing penetration depth.
4. The chamfer corroded by the electrolyte will be larger. Thus, after using for a long time, the anodes with a larger chamfer will cause larger penetration depth.
5. By analyzing experimental data with dimensional analysis method, the penetration depth's dimensionless equation relating to physical factors, operating factors and equipment factors is obtained:

$$\frac{A}{H} = 0.0005439\left(\frac{\Delta\rho Q^2}{H^3\sigma}\right)^{0.236055}\left(\frac{d}{H}\right)^{-0.268231}\left(\frac{h}{H}\right)^{1.782124}$$

After analysis, the dimensionless equation about the influence of gas flow rate on the penetration depth is obtained.

$$A = 0.001351Q^{0.47211}d^{-0.268231}$$

The dimensionless equation about the influence of electrolyte level on the penetration depth is:

$$A = 0.034539d^{-0.268231}h^{1.782124}$$

ACKNOWLEDGEMENT

This research was supported by the National Natural Science Foundation of China (No. U1202274), the National High Technology Research

and Development Program of China (No. 2012AA062303) and the Specialized Research Fund for the Doctoral Program of Higher Education of China (No. 20120042110011).

REFERENCES

1. N.X. Feng, X.Q. Qi, and J.P. Peng, *Chin. J. Nonferr. Met.* 15, 2047 (2005).
2. J.P. Peng, N.X. Feng, Y.-L. Jiang, Y.-W. Wang, and J. You, *Chin. J. Nonferr. Met.* 18, 738 (2008).
3. H. Yue, *J. Mater. Metall.* 9, 44 (2010).
4. T. Yingfu, *J. Light Met.* 2, 31 (2011).
5. N.X. Feng, F.Q. Tian, Y.L. Xu, and Y. Shu, *J. Light Met.* 7, 29 (2000).
6. J. Zoric and A. Solheim, *J. Appl. Electrochem.* 30, 787 (2000).
7. J.L. Xue and H.A. Oye, *Light Metals 1999*, ed. C.E. Eckert (Warrendale, PA: TMS, 1999), pp. 247–253.